

Removal of Methylene Blue Dye from Aqueous Solution on to Novel Adsorbents: Molybdenum Dicarbonate-Filter Paper and Molybdenum Dicarbonate-Activated Carbon Composites

Ferooze Ahmad Rafiqi*, Shabir Ahmed Bhat and Raveed Yousuf Bhat

Govt. Degree College Anantnag, Department of Higher Education, Jammu and Kashmir, India.

ARTICLE INFO

Article history:

Received: 15 March 2023;

Received in revised form:
1 May 2023;

Accepted: 10 May 2023;

Keywords

Molybdenum Dicarbonate;
Filter Paper;
Activated Carbon;
Adsorption;
Wastewater Treatment.

ABSTRACT

Two composites-1) Molybdenum dicarbonate-filter paper and 2) Molybdenum dicarbonate-activated carbon were synthesized and characterized by X-ray diffraction (XRD), scanning electron microscopy (SEM) and energy dispersive X-ray analysis EDX. Using the method of UV-visible spectroscopy, the removal efficiencies and adsorption capacities of these composites towards the removal of methylene blue (MB) from aqueous solution were compared. The findings of the MB adsorption with these composites (I and II) indicated equilibrium adsorption in less than 5 minutes. Composites I and II have MB removal efficiencies of 87% and 96.25%, respectively, and their estimated adsorption capacities at 20°C are 432 mg g⁻¹ and 481 mg g⁻¹. The adsorption process of MB onto Molybdenum dicarbonate-filter paper (composite I) suited well with the pseudo-first order and pseudo-second order kinetics and conformed to intraparticle diffusion model for Molybdenum dicarbonate-activated carbon composite (composite II). Adsorption of MB onto composite I aligned with both Freundlich model and Tempkin models due to higher values of correlation coefficients and fitted well with Langmuir model for composite II. Adsorption process was found to be endothermic and spontaneous in nature. The adsorption results revealed that these composites could be employed as effective adsorbents to remove dyes from industrial effluents.

© 2023 Elixir All rights reserved.

1. Introduction

Freshwater fit for drinking on earth is less than 1.5 percent of the total earth's 3 percent freshwater quantity[1]. To cater the water requirements of 8 billion people with this meagre amount of drinking water is undoubtedly a great challenge for this century. This problem has been further exacerbated due to the impacts of climate change. The manufacturing industries especially the textile industries consume unmeasurable quantity of water that generates tonnes of effluents which require advanced technologies for treatment and purification[2].

Dyes and pigments used in textile industry are water-intensive as very large amount of water is consumed during the dyeing of fabrics. At an average, 10⁷ Kg of dyes are consumed per year out of which 10⁶ are discharged into waste streams alone by textile industry [3]. One Kg of textile requires 200L of water at an estimated approximation. This dyeing of textiles thus further adds the existing deteriorated drinking water scenario of the world.

More than 10,000 dyes and pigments are used worldwide out of which methylene blue (MB) is amongst the most commonly used dye[4]. In this work, we have picked Methylene blue (MB) dye and investigated it as a test probe for remedial experiments. Methylene blue is mainly used as a dye in textile, printing, food industries and distilleries[5], besides being employed as a chemical indicator and ISO test pollutant in semiconductor photocatalysis[6]. Although this dye has some medicinal and pharmaceutical applications [7, 8] but its release in water bodies poses threat not to aquatic

ecosystem but to human beings too[9]. MB molecule has an aromatic structure thus rendering it poor biodegradability. This dye imparts color to the surface water thus reduces the penetration of sunlight depriving the algae to undergo normal photosynthesis. This dye increases the chemical oxygen demand in the water besides triggering bioaccumulation in human food chain [10-12]. MB engenders different diseases in human beings like gastrointestinal tract infection, dermatitis, Heinz body formation, quadriplegia, jaundice, allergy and can stimulate mutations in human beings [13-15], thus it has serious environmental concerns. It is now essential for industrialists, chemists, and environmentalists to decontaminate it in wastewater streams and reduce its utilisation in industry in order to accomplish sustainable water management and to preserve a healthy and environment-friendly life structure on earth. Various chemical, physical and biological methods were used worldwide in scavenging the dyes and pigments, heavy metals and other toxins from industrial effluents and other real water samples and sources. These methods include membrane filtration, reverse osmosis, flocculation, sedimentation, liquid-liquid extraction, dialysis, biological oxidation and adsorption[16-20]. Among the listed methods, adsorption is the most efficient and reliable physicochemical treatment method of heavy metal and dye-bearing wastewater[21-23]. This is because of good economics, simple procedure, simplicity of design, environment-friendly and efficient method amongst the all methods available.

Adsorbents based on agricultural waste that are non-conventional and renewable sources have received considerable attention in dye-bearing wastewater treatment from last few decades. The use of bioresource as adsorbents is still in vogue and are demanded by the research community globally because of their low cost, abundance, easily available, high adsorption capacity than conventional adsorbents and high selectivity towards toxins [24-26].

As per the research findings over the use of biowaste material as adsorbents are concerned, some prominent examples are pine-fruit shell, spent coffee, tree fern, palm oil mill effluent waste, orange peel, rice husk, orange peel, wheat shells, corn husk, bamboo dust, sugar beet pulp, spent tea leaves, seeds, Shorea roxburghii, saw dust and catha edulas stem [5,6,9,11-14, 16]. Almost every part of the plant/tree has been tested as adsorbent and have proven as efficient materials for waste water treatment [27-31]. These agricultural wastes and other bioresource materials are used with slight or heavy physical and chemical modifications. These changes include carbonation, acid-alkali hydrolysis, bleaching and extracting methods, drying, ultrasoication, heating under different condition and various physical processes [4-6, 9-13]. The fundamental components produced by diverse physical and chemical processes on agricultural and forestry products are cellulose and activated carbon. After processing, these materials are made accessible for commercial sale. Powdered activated charcoal and filter paper are two examples.

In this study, the cellulose chains of filter paper were doped with molybdenum dicarbonate (MoC_2O_6), and the activated carbon was likewise blended with the same complex. Applications for molybdenum complexes are numerous in research and technology [32-34]. The uncoordinated lone pairs on the two oxygen atoms in this complex can impart a basic character in them, which is the major reason for employing it as a component in the composite formation. These composites are good candidates for use as adsorbents in the wastewater treatment process for the removal of cationic dyes like MB due to their basic nature. The efficiency removal percentage of these prepared composites are much higher than various reported results. This is supported by the fact that employing these new composites, 96.25% and 87% of MB are removed from an aqueous solution within 5 minutes at 20°C.

The principal objectives of this study are: (1) successful synthesis of Molybdenum dicarbonate (MoC_2O_6)-filter paper composite and MoC_2O_6 modified activated carbon, (2) Use of these composites as adsorbents towards the removal of MB from aqueous solutions and to examine their adsorption capacities, (3) To investigate the effects of contact time, dosage, pH, temperature and concentration of MB on the adsorption behaviour, and (4) to evaluate different kinetic and thermodynamic parameters.

2. Experimental

2.1. Materials

Ammonium molybdate $\{(\text{NH}_4)_2\text{MoO}_4\}$ of Merck quality and methylene blue (MB) of Qualigens chemicals were used. Whatman filter paper and powdered activated charcoal were purchased from Loba chemicals and utilised exactly as received from the supplier. MB has the chemical formula $\text{C}_{16}\text{H}_{18}\text{N}_3\text{SCl}$. It dissolves in water at a rate of 43.2 g/L at 20 °C, and when MB is dissolved in water, a blue cationic dye is generated. In its canonical structure, it has a positive charge either on nitrogen or sulphur. Sodium Carbonate, ethanol and ammonia were also supplied by Loba chemicals. In the synthesis and experimentation part, doubly distilled water was used.

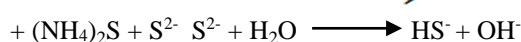
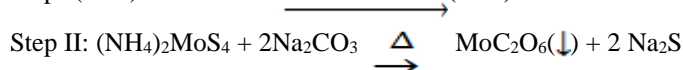
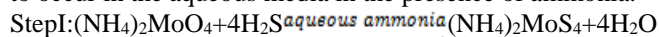
2.2. Instrument and measurements

The Kipps apparatus was used for the production of hydrogen sulphide gas. XRD data was obtained using PW 3050 base diffractometer with CuK_α radiation of 1.540598 Å. Surface morphology of the samples were carried out on ZEISS EVO series scanning electron microscope model EVO50. The textural properties were determined by N_2 adsorption desorption at 75 K using an ASAP 2420 system by Brunaur-Emmet-Teller method. Energy dispersive X-ray (EDX) of Bruker model was resorted to investigate the elemental composition of molybdenum complex and its successful insertion into the synthesized composites. In order to determine the maximum wavelength of MB, equilibrium concentration and adsorption kinetics, Ultraviolet-visible (UV-vis) spectra were taken on double beam UV-Visible spectrophotometer T 80. This spectrophotometer has a scan range of 200-1100 nm wavelength and a cell of 1cm optical path length.

2.3. Synthesis

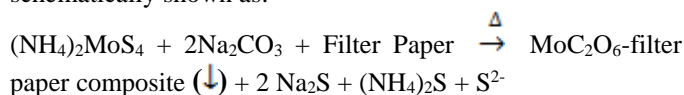
2.3.1. Synthesis of Molybdenum dicarbonate (MoC_2O_6)

Using a magnetic stirrer, 49 grams of the salt is dissolved in 250 ml of distilled water to create a 1 M ammonium molybdate solution. In the presence of 10 ml of ammonia, the hydrogen gas generated by the Kipps device is passed through this molybdate solution. This mixed solution is added a 1 M sodium carbonate solution. The entire solution has been heated at 60°C for 30 minutes. Crystals of a dark crimson colour are precipitated. The solution is filtered and repeatedly rinsed with ethanol after standing for 24 hours. The sample is desiccated for 48 hours after being dried in an oven at 90 °C. A little portion of the synthesis was completed using well-established synthesis techniques [35]. The following reactions are expected to occur in the aqueous media in the presence of ammonia.



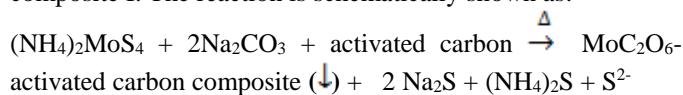
2.3.2. Synthesis of Molybdenum dicarbonate (MoC_2O_6)-filter paper Composite:

The Whatman filter papers were cut into pieces that were 1 mm in size. 1g of these cut pieces are then added to the mixture solution during the step II of the procedure of Molybdenum dicarbonate synthesis. After standing in the solution for 24 hours, it is filtered. The sample obtained during filtration is cleaned with ethanol, then dried in an oven at 50 °C, followed by 48 hours of desiccation. The reaction is schematically shown as:



2.3.3. Synthesis of Molybdenum dicarbonate (MoC_2O_6)-activated carbon Composite:

In this composite formation, 1g of activated carbon is added to the mixture solution during the step II of the synthesis of Molybdenum dicarbonate. The same procedure has been adopted for the separation of sample as adopted for composite I. The reaction is schematically shown as:



2.4. Adsorption experiments

In the adsorption experiments, the following procedure was adopted. 50 mg of MB was added to 100 ml of doubly distilled water and 10 ml of this stock solution was then treated with 100 mg of MoC_2O_6 -filter paper composite

(composite I) and MoC₂O₆-activated carbon composite (composite II), separately. The solutions were manually agitated for a short span of time (1 minute). Then simple decantation process was used for the removal of adsorbent and the decant was examined for the unadsorbed MB, spectrophotometrically using the double beam spectrophotometer. Absorption spectra of MB were taken after every one minute time interval. Concentrations of MB was calculated using the equation of Lambert-Beer's Law:

$$A = \epsilon bc \quad (1)$$

Where A, b and c are the absorbance, thickness of the cell and concentration of the MB in the solution, respectively. ϵ is molar extinction coefficient which is constant for a particular species at a particular temperature.

3. Results and discussion

3.1. SEM-EDS Characterization

Fig.1. (a-c) shows the SEM images of Molybdenum dicarbonate (MoC₂O₆), Molybdenum dicarbonate (MoC₂O₆)-filter paper (composite I) and Molybdenum dicarbonate (MoC₂O₆)-activated carbon (Composite II), respectively. SEM image of Molybdenum dicarbonate mostly shows rectangular mass of crystals indicating the agglomeration of molybdenum dicarbonate molecules. The SEM images of composites show the presence of molybdenum dicarbonate crystals on the surfaces of filter paper and activated carbon in the composites. Activated carbon shows the honey comb like structure within pores of which Molybdenum dicarbonate crystals are visible. The interaction between the components looks superficial that indicates the van der waal's type of interaction between them. The composite formation is further substantiated with the EDS spectrum that shows prominent peaks of molybdenum, carbon and oxygen as shown in Fig.2. (a-c). Weight percentage of Mo, C and O present in the Molybdenum dicarbonate are 45%, 12.20%, 20.92%, respectively. The composite with filter paper shows weight percentage of Mo, C and O 28.19%, 28.7% and 38.73%, respectively. The composite of Molybdenum dicarbonate with activated carbon shows weight percentage of Mo, C and O 33.72%, 53.19 %, and 10.82 %, respectively.

The textural properties viz. specific surface area and average pore diameter size of both the composites were calculated via BET method. Surface area of composite I is found to be 64 m²/g while as this value for composite II is 1654 m²/g. This indicates that the powdered charcoal has almost 26 times more surface area than that of filter paper in unit mass of their substances. The average pore diameter of composite I is 3.0-5.0 nm while as this value ranges 2.5-4.0 nm for composite II.

3.2. XRD Characterization

X-ray diffraction (XRD) analysis were carried out on PW-3050 base diffractometer with Cu K α radiations in the scanning range of 0°-80°. Fig.3. (a-c) shows the XRD diffraction pattern of (a) Molybdenum dicarbonate (dopant), (b) Molybdenum dicarbonate-filter paper and (c) Molybdenum dicarbonate-activated carbon composite, respectively. The XRD patterns of the dopant and the composites confirms the crystallinity of the samples. The Molybdenum dicarbonate-Whatman filter paper exhibits semicrystalline peaks at 16.47 and 22.5, which are the characteristics peaks shown by cellulose structure of paper [36]. Besides these characteristic peaks, peaks at 2 θ values of 11.47, 27.20, 34.33 and 46.83 are observed in the XRD pattern of this composite which is likely because of the metal complex component of the composite. Two wide peaks at 25.04° and 43.98° are the prominent amorphous peaks of activated carbon. In the XRD pattern of

the composite of activated carbon, some sharp peaks at 2 θ values of 17.91, 27.20, and 33.62 have been observed which is due to the molybdenum dicarbonate component. Sharp peaks are the characteristics of crystalline substances [22], the appearance of such type of peaks in both the methyl dicarbonate and composite proves the crystalline nature of the composites. The peaks of methyl dicarbonate are appearing in both the composites with appreciable shifts that supports a good interaction between the components and confirms the successful synthesis of composites of methyl dicarbonate with whatman filter paper and activated carbon.

3.3. Efficiency removal

The following equation is generally employed to determine the percentage removal efficiency of adsorbents (composite I and II) towards the removal of dyes (MB) and heavy metals:

$$\eta = (C_i - C_t) / C_i \times 100 \quad (2)$$

Where C_i and C_t are the initial concentration of MB and its concentration at time 't', respectively. The concentration terms are expressed in mgL⁻¹.

The following equation has been used to determine the maximum adsorption capacity of the adsorbents (composite I and II) :

$$Q_e = \left(\frac{C_i - C_e}{M} \right) V \quad (3)$$

Where C_i and C_t are the initial concentration of MB and its concentration at time 't', V is the volume of solution (L), and M is the mass of adsorbent (g), Q_e is maximum adsorption capacity of the adsorbent, expressed in mg/g.

3.3.1. Effect of contact time

Absorption spectra of Methylene blue adsorption by (a) Molybdenum dicarbonate (b) Molybdenum dicarbonate-filter paper and (c) Molybdenum dicarbonate-activated carbon composite, respectively, are shown in Fig.4. Absorbance of MB solutions is measured by UV-visible spectrophotometer. MB in aqueous solution exhibits maximum absorbance at 662 nm. Concentration of MB in the given aqueous solution decreases upon addition of the adsorbents. MB is removed from aqueous solutions probably through electrostatic interactions as the MB is cationic in nature. Porous nature of filter paper and activated carbon could augment the adsorption of MB.

Molybdenum dicarbonate-filter paper and Molybdenum dicarbonate-activated carbon composite have shown excellent adsorption capacities due to the synergy of Molybdenum dicarbonate and basic matrices of filter paper and activated carbon. Molybdenum dicarbonate-activated carbon composite is better adsorbent than Molybdenum dicarbonate-filter paper that is probably due to the high specific area of the activated carbon. Adsorption of 96.25% MB on the composite II and 87% on the composite I occurs within 5 minutes duration at room temperature. The adsorption efficiency removals of these composites were determined as per equation (2). However, a slight increase in the adsorption of MB onto composite I and II occurs on increasing the contact time from 5 minutes to 60 minutes. The maximum adsorption capacity of composite I and II are calculated using the equation (3) and the values are 432 mg g⁻¹ against composite I and 481 mg g⁻¹ against composite II. These adsorbents are excellent candidates for potential industrial applications due to their high adsorption capacities. The results are summarised in Table 1 and show that these composites have greater adsorption capabilities than activated carbon and unmodified filter paper. These higher values of composites than the neat matrices vindicate the role of molybdenum dicarbonate in

improving the sequestration potential of these prepared composites towards the MB removal. However, unmodified activated carbon shows better removal efficiency than the neat filter paper on account of its high specific area. The order of adsorption capacities follow the order: Molybdenum dicarbonate-activated carbon composite, Molybdenum dicarbonate-filter paper, Molybdenum dicarbonate complex.

The maximum adsorption capacities for MB by these adsorbents are either higher than some research findings or competitive to among the best adsorbents reported so far. The data reported in the literature is shown in Table 2. [37-46, 2,4, 6,9,10,13,15,21,23]. Molybdenum dicarbonate-filter paper and Molybdenum dicarbonate-activated carbon composite having oxygen atoms with uncoordinated lone pair of electrons can easily bind MB through electrostatic interaction. These oxygen atoms may belong either to Molybdenum dicarbonate component or the -OH function group of cellulose chains of filter paper. Further the MB molecules can be entrapped within the micro and mesopores of the composites [24-31]. The mechanism of adsorption of MB on composite I and II involves more than one type of interactions. However, electrostatic attraction between oppositely charged sites plays a dominating rule in the adsorption of MB. Molybdenum dicarbonate with uncoordinated lone pair of electrons on oxygen atoms makes the composite I and II an exclusively electron rich substrates where cationic dyes like MB can be easily lured and bound. This property makes these composites an ideal candidate for cationic dye removal in real wastewater samples. The hydroxyl and oxygen units of cellulosic part of paper also enhances the adsorption capacities towards the cation dye MB molecules.

3.3.2. Effect of initial concentration of MB dye

About 87% and 96.25% of the adsorption of MB onto composite I and composite II occurs within 5 min. This can be both because of the (i) electrostatic attraction between the cationic MB dye molecule and oxygen atoms of methyl dicarbonate (ii) Interaction between MB with hydroxyl groups of filter paper and (ii) also due to trapping of MB molecules within pores of the composites. With the increase in the concentration of MB, the adsorption gradually decreases. This may either be because of the full occupancy of active sites or the agglomeration of MB dye molecules. Aggregated MB molecules further can disperse the individual free molecules to move deeper inside the porous core of the composite. Under the same initial dye concentration, the adsorption capacity of composite II is better to that of composite I as shown in Table 3. This may be because of the large specific surface area and higher porous density of composite II.

3.3.3. Effect of pH

The adsorption of MB onto the composite I and composite II varies with the pH of the solution. Both composite I and composite II show excellent adsorption at pH 7 and less adsorption in alkaline solution and least in acidic solution. At low pH, uncoordinated oxygen atoms of molybdenum dicarbonate and hydroxyl of cellulosic part of filter paper are highly protonated, thus, develops a positive charge throughout the adsorbent, therefore, shows low adsorption affinity towards MB elimination from the conc. HCl solution. At higher pH, OH-ions affects the free motion of cationic MB molecule because of electrostatic neutralization, thereby makes their attraction a bit low towards the active sites of adsorbents. The results obtained are summarized in Table 4. The order of removal of MB by the adsorbents follows the order: Neutral medium, alkaline medium, acidic medium.

3.3.4. Effect of adsorbent dosage

Fixed quantity of MB aqueous solution (10 ml of 50 mg L-1 MB) is treated separately with adsorbents (composite I and II) in the quantity ranging from 100-500 mg in the increments of 100 mg. Adsorption of MB onto these composites are then investigated at each dose of adsorbent. The removal percentage of MB from aqueous solution increases with the increase in the amount of adsorbent dose. It is mainly because of the increase in the number of active sites, surface area and also because of increase in pore number of adsorbents. Molybdenum dicarbonate having uncoordinated oxygen atoms provides binding sites to positively charged MB molecule. The removal efficiency is higher for composite II as compared to Composite I at all adsorbent dose levels that might be because of large surface area of the composite II.

3.3.5. Effect of Temperature

50 mg of MB was dissolved in 1L of doubly distilled water. 10 ml of this stock solution was treated separately with 100 mg of composite I and II for a contact time of 5 minutes at 20°C. It was then decanted and the decant part was examined by UV-visible spectroscopy. Stock solution was heated to 40°C, 60°C, 80°C and 100°C and at each temperature, the above procedure was adopted (10 ml of stock solution treated with 100 mg adsorbent). Adsorption of MB onto both composites continuously increased from 20°C to 80°C due to the enhanced thermal motion of MB particles in the aqueous solution and the adsorption capacities at different temperatures are shown in Table 5. At 100°C, adsorption starts decreasing to a little extent indicating the commencement of desorption phenomenon of MB molecules.

3.4. Adsorption kinetics

The following pseudo-first-order equation which is also known as Lagergren first order rate equation is based on concentration of the solution and adsorption capacity of the solid:

$$\log(Q_e - Q_t) = \log Q_e - \frac{K_1}{2.303} t \quad (4)$$

The following pseudo-second-order rate expression is also based on the adsorption capacity of solids:

$$\frac{t}{Q_t} = \frac{1}{K_2 Q_e^2} + \frac{t}{Q_e} \quad (5)$$

The intra-particle diffusion model described by Weber and Morris is based on the concentration of adsorbate 'C' expressed in mg L-1 and is represented by the following equation:

$$Q_t = k_1 t^{1/2} + C \quad (6)$$

Where k_1 , k_2 and k_i are rate constants for pseudo-first-order, pseudo-second order and intra-particle diffusion models, respectively. Q_e and Q_t represents the adsorption capacity (amount of MB adsorbed per unit mass of adsorbent) at equilibrium and at time 't' and is expressed in mg g⁻¹.

Pseudo-first order, pseudo-second order and intra particle diffusion models are used to describe the kinetics of MB adsorption reactions. Linear equation analysis viz; $\log(Q_e - Q_t)$ vs. t, t/Q_t vs. t and Q_t vs. $t^{1/2}$ predict the validity of these models in the kinetics of adsorption reactions.

The fitting plots for pseudo-first order, pseudo-second order and intraparticle diffusion models are shown in Fig. 5, 6 and 7, respectively. Based on the values of correlation coefficients (R²) obtained from fitting results as shown in Table 6, the pseudo-first order and pseudo-second order are used as suitable models to describe the adsorption of MB onto composite I (Molybdenum dicarbonate-filter paper) and intraparticle diffusion model for the composite II

(Molybdenum dicarbonate- activated carbon). The value of k_1 (min^{-1}) for composite I and II are 0.4675 and 0.5158 respectively while as Q_e values come out as 607 and 582 (mg g^{-1}) for these composites. However there is no concordance in the experimental and calculated Q_e values, therefore the adsorption of MB onto these composite via pseudo-first order kinetics is not wholesome. The value of Q_e , k_2 and h obtained from fitting results of pseudo-second order kinetic equation for composite I and II have been found identical and the values for these parameters are 1000 (mg g^{-1}), 5×10^{-4} (min^{-1}) and 500 $\text{mg (g min}^{-1})$, respectively. These identical values suggest the equivalent effect of Molybdenum dicarbonate on the matrices of filter paper and activated carbon.

The intraparticle diffusion model is also used to investigate the kinetics of MB onto composite I and II. The value of k_i for composite I is 165.7 $\text{g (mg min}^{-1})$ and for composite II is 182.5 $\text{g (mg min}^{-1})$. C_e for Composite I and II are observed as 70.53 and 57.63 mg L^{-1} , respectively. The concordance in the experimental and calculated C_e values (50 mg L^{-1} and 57.63 mg L^{-1}) in case of composite II suggests the adsorption of MB onto composite II via intraparticle diffusion model. This statement is further buttressed with good R^2 value of 0.972 which is 0.963 for composite I.

3.5 Adsorption isotherm

Langmuir model 2) Freundlich model and 3) Tempkin model are used to investigate the adsorption isotherm of MB onto composite I and II. The linearized Langmuir, Freundlich and Tempkin plots of MB adsorption by composite I and II are shown in Fig. 8, 9 and 10, respectively.

The following equation of Langmuir model is used to determine the equilibrium concentration of the adsorbate and the Langmuir adsorption constant:

$$\frac{C_e}{Q_e} = \frac{1}{K_L Q_{\max}} + \frac{C_e}{Q_{\max}} \quad (7)$$

Where Q_{\max} is the maximum adsorption capacity at saturation (mg g^{-1}), C_e the equilibrium concentration of the adsorbate (MB) and K_L is the Langmuir adsorption constant and that is related to the energy of adsorption.

The Langmuir adsorption isotherm parameters Q_{\max} and K_L calculated from the slope and intercept of the linear equations for composite I are 250 mg g^{-1} and 0.142 (L g^{-1}), respectively while as these values are 250 mg g^{-1} and 0.111 g L^{-1} for composite II. R^2 value for composite II is higher than composite I, suggests the adsorption of MB onto composite II via chemisorption and formation of monolayer coverage of MB on the adsorbent can be predicted. Molybdenum dicarbonate due to the presence of uncoordinated oxygen atoms binds the cationic dye via Lewis acid-Lewis base interaction thereby improves the adsorption capacity of the composite material further.

The following equation of Freundlich model is used to determine the Freundlich adsorption constant:

$$\ln Q_e = \ln K_F + \frac{1}{n} \ln C_e \quad (8)$$

Where Q_e is the maximum adsorption capacity of adsorbent (mg g^{-1}), C_e the equilibrium adsorbate concentration, n is the Freundlich constant, K_F is the other constant related to the maximum adsorption capacity.

The following equation of Tempkin model is used to determine the equilibrium binding energy constant:

$$Q_e = B \ln KT + B \ln C_e \quad (9)$$

Where KT is the equilibrium binding energy constant and B is a constant related to the energy of adsorption.

Adsorption of MB is not restricted to Langmuir type of interactions only as R^2 value for both composites I and II have been found exceeding 0.75 in Freundlich and Tempkin models. The isothermic parameters are summarized in Table 7. K_F value for composite I comes out 6.16×10^6 and 19.68×10^6 for composite II. The KT values obtained after fitting the plots are also very high. This parameter is 1.12×10^6 for composite I and 5.49×10^5 for composite II. The higher values of K_F and KT for both these composites endorse the role of these models in investigating the adsorption isotherm of MB onto these composites. The hydroxyl groups of filter paper and uncoordinated lonepairs available on molybdenum dicarbonate moieties can pick up cationic MB molecules through electrostatic interactions. Such type of adsorbate and adsorbent interactions are of chemisorption natures. However the porous nature of filter paper and activated carbon components can facilitate the adsorption of MB via physisorption. Thus the adsorption mechanism between MB and these composites involves both physisorption and chemisorption phenomena.

3.6 Thermodynamic Study

The values of thermodynamic parameters like change in entropy (ΔS°), enthalpy change (ΔH°) and standard Gibbs free energy change (ΔG°) for the adsorption of MB from aqueous solution onto composites I and II are summarized in Table 8. The following equations (10 & 11) are used to calculate these parameters.

$$\ln (Q_e/C_e) = \frac{\Delta S^\circ}{R} + -\Delta H^\circ/RT \quad (10)$$

where Q_e is the maximum adsorption capacity of adsorbents (mg g^{-1}), R is gas constant ($\text{J K}^{-1} \text{mol}^{-1}$) and T is the temperature. The term $\ln (Q_e/C_e)$ of Van't Hoff equation (10) is termed as adsorption affinity. Plotting $\ln (Q_e/C_e)$ vs. $1/T$ as shown in Fig.11, the values of ΔS° and ΔH° are obtained from the intercept and slope of the fitted line plot, respectively.

ΔG° is calculated by the following Gibbs-Helmholtz equation.

$$\Delta G^\circ = \Delta H^\circ - T\Delta S^\circ \quad (11)$$

The touchstone for a reaction to occur via physisorption, hydrogen bonding interaction or a chemisorption is predicted and described by Rehman et al.[47]. As per the stated authors [47], the ΔH° value for physical adsorption is 4-10 KJ mol^{-1} . The ΔH° value for Hydrogen bonding forces are 2-40 KJ mol^{-1} and it is greater than 40 KJ mol^{-1} for chemical adsorption type of reactions.

The ΔH° value for adsorption of MB on composite I is 6.453 KJ mol^{-1} and onto composite II is 8.779 KJ mol^{-1} . These results suggest that the adsorbate (MB)- adsorbent interactions correspond to physisorption type. Another standard for predicting the type of adsorption is the value of standard free energy change (ΔG°). For physical adsorption, ΔG° lies in between -20 to 0 KJ mol^{-1} and this value for chemical adsorption ranges in between -80 and -400 KJ mol^{-1} [48]. The ΔG° value for the MB adsorption onto composites I

and II also establishes the interactions between MB and adsorbents a physisorption one and also spontaneous in the temperature range from 20 °C to 80 °C. The ΔG° values from 20 °C to 80 °C ranges from -5.994 to -8.544 KJ mol⁻¹ for composite I and -6.132 to -9.085 KJ mol⁻¹ for composite II.

As the value of enthalpy change (ΔH°) comes out positive, this shows the endothermic nature of the adsorption process. A positive value of entropy change (ΔS°) indicates disorderliness at the solid/liquid interface so the adsorption of MB onto these composites is an entropy driven spontaneous process and the spontaneity of the adsorption processes are further substantiated with the negative value of ΔG° . The removal of MB (per unit mass of adsorbent) from aqueous solution increases imperceptibly with increase in temperature upto 80 °C beyond which a small decrease in the removal of MB occurs as already discussed in section 3.3.5 (Effect of Temperature). This increase could be because of the enhanced thermal motion of MB molecules and a decrease in the solute solvent interaction upto 80 °C. Temperature onwards 80°C, desorption would likely to occur. Thus these adsorbents have better removal efficiency of MB from aqueous solutions upto higher temperature limit of 80 °C.

4. Conclusion:

(i) Molybdenum dicarbonate-filter paper and activated carbon composites can be used as efficient adsorbents in waste water treatment due to their high efficiency removal and adsorption capacities over a wide range of temperature. At 20 °C, composite I and II shows MB removal efficiency percentage of 87 and 96.25

(ii) The amount of MB removal increases from aqueous solution both by increasing the adsorbent dosage (100 to 500 mg) as well as the initial concentration of MB (50-80 mg L⁻¹).

(iii) Maximum removal of MB occurs at pH 7 within 5 minutes of contact time.

(iv) Removal of MB from the aqueous solution using these composites increases with increase in temperature from 20 to 80 °C probably due to higher thermal motion of dye molecules.

(v) Adsorption of MB onto composite I conform with pseudo-first order and pseudo-second order kinetics due to good regression values of R² whereas composite II suited well with Intraparticle diffusion model.

(vi) Adsorption of MB onto composite I aligned with Freundlich and Tempkin models due to higher regression values of R² whereas composite II fitted well with Langmuir isothermic model.

(vii) Adsorption of MB onto composite I and II are spontaneous and endothermic.

Acknowledgements

We would like to express our gratitude to the research institution of Sophisticated Analytical Instrumentation Facility Sophisticated test and instrumentation centre (SAIF STIC) Kochi for providing the instrumentation facilities. The authors are thankful to two Lab. Bearers Mr. Owaise Ahamad and Mr. Sameer Khalil Dar and Head of the Department of Chemistry, GDC Anantnag, Prof Fayaz Ahmad Bhat, for their support and cooperation in accomplishing the basic experimentation part of this research work.

Funding

Not applicable.

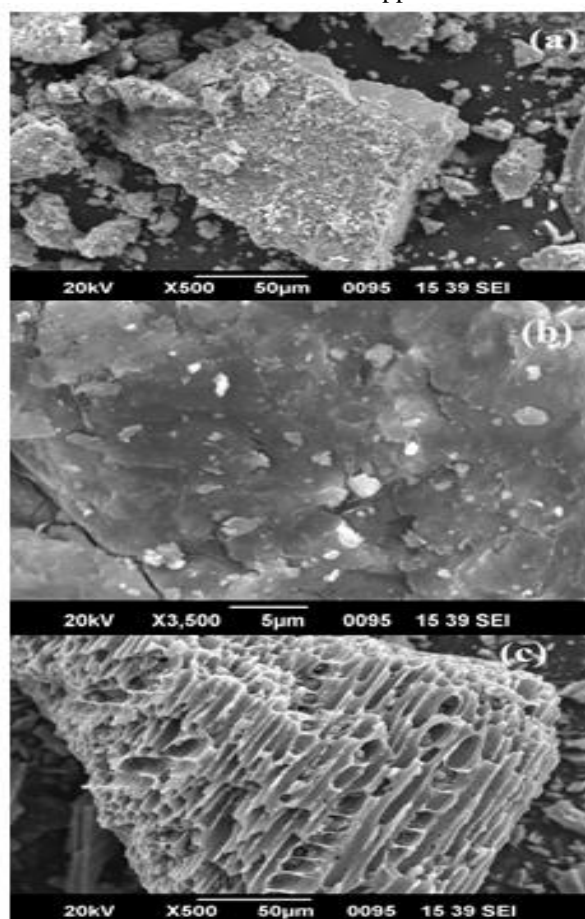


Fig 1. SEM images of (a) Molybdenum dicarbonate, (b) Molybdenum dicarbonate-filter paper and (c) Molybdenum dicarbonate-activated carbon composite.

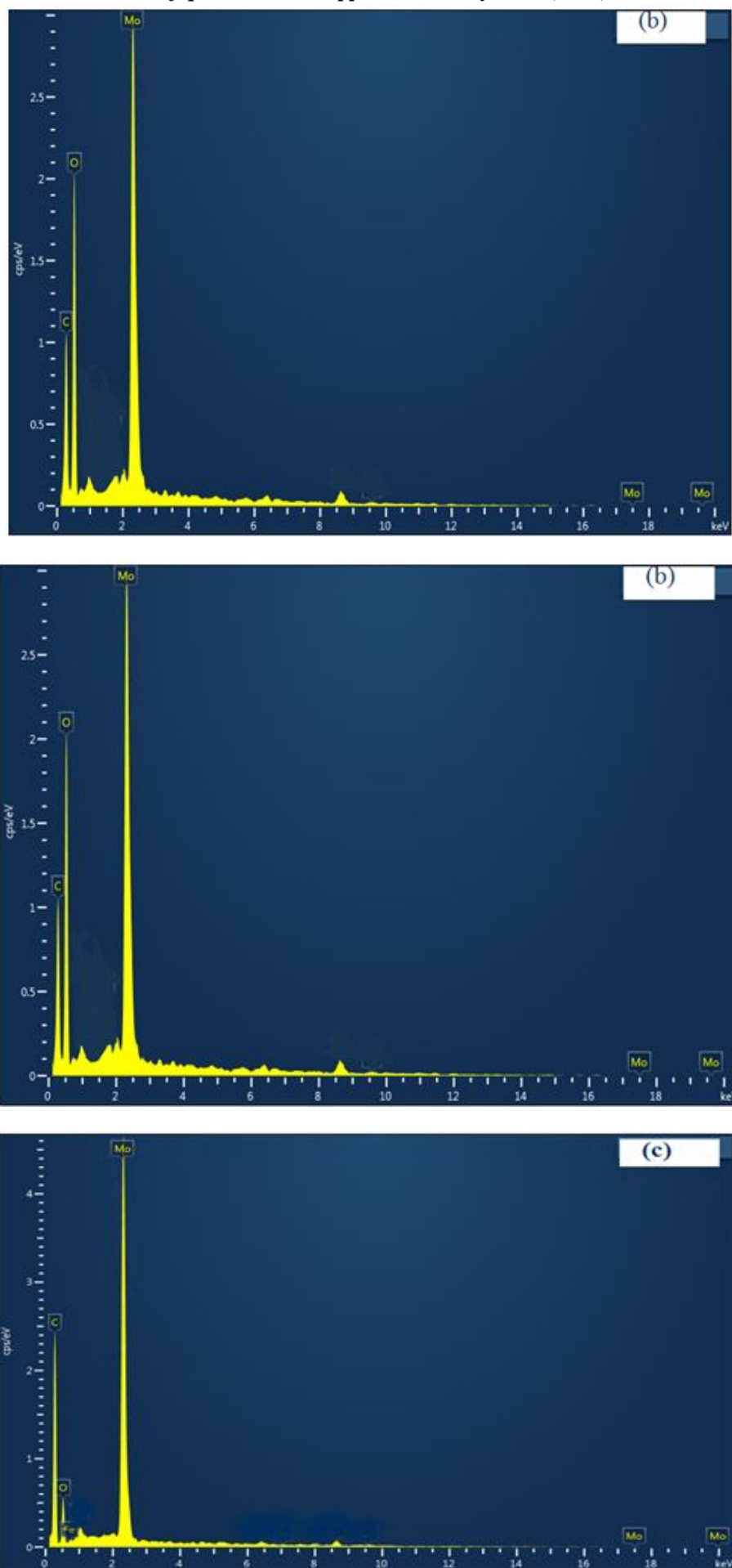


Fig 2. EDS spectrum of (a) Molybdenum dicarbonate, (b) Molybdenum dicarbonate-filter paper and (c) Molybdenum dicarbonate-activated carbon composite.

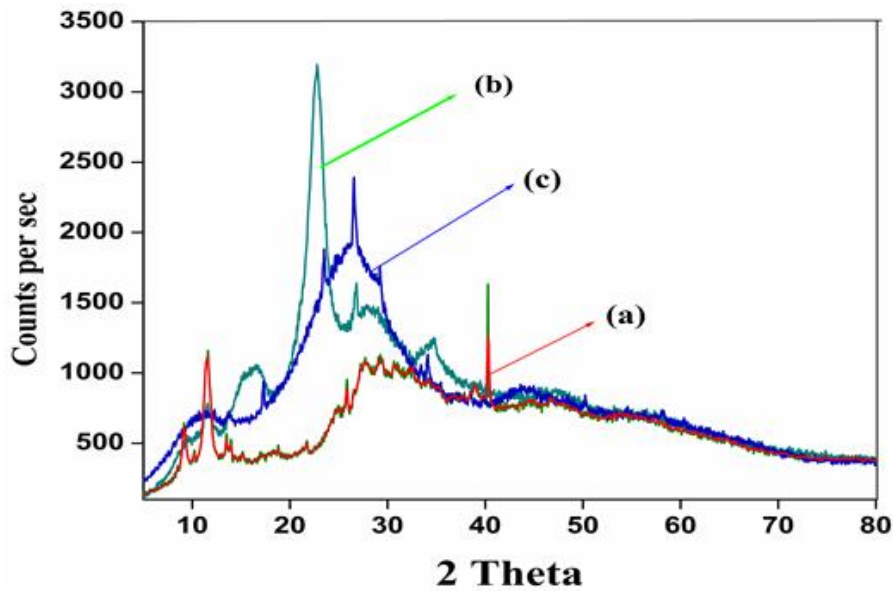


Fig 3. XRD spectrum of (a) Molybdenum dicarbonate, (b) Molybdenum dicarbonate-filter paper and (c) Molybdenum dicarbonate-activated carbon composite.

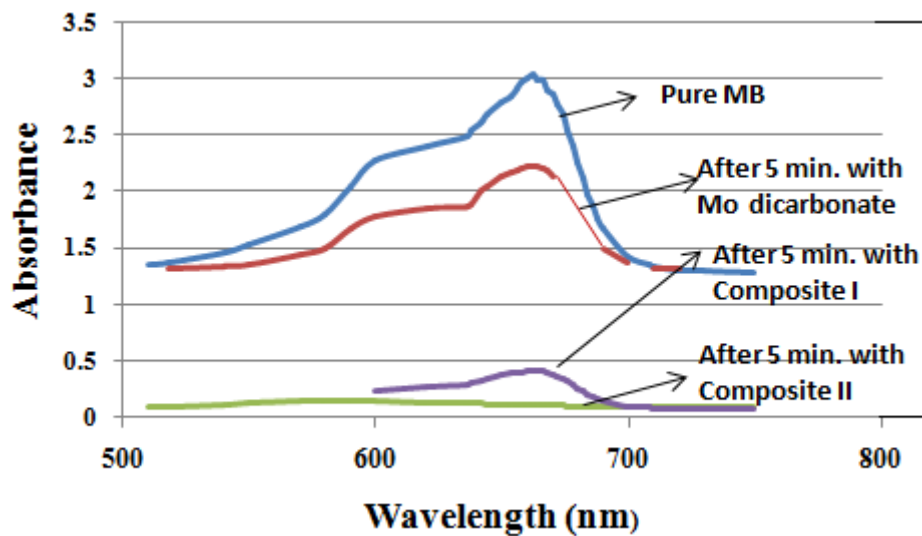


Fig 4. Visible spectra of MB aqueous solution treated with composites I and II at room temperature.

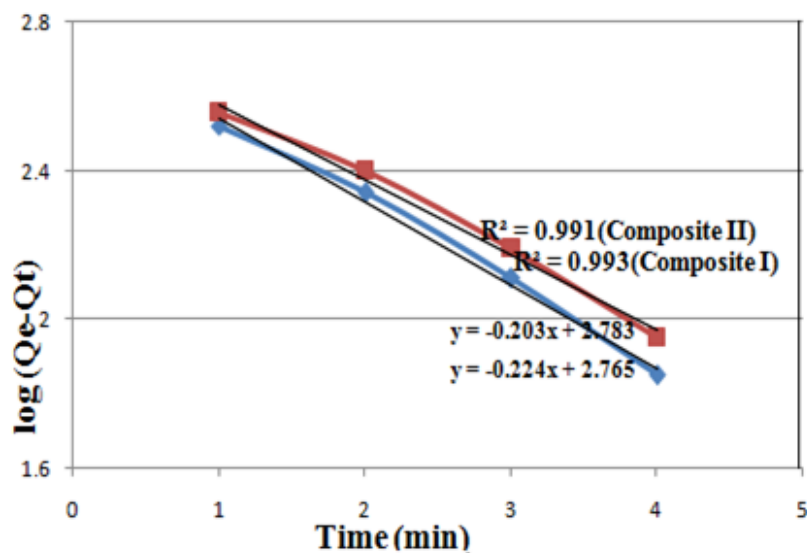


Fig 5. Pseudo-first order plot for MB adsorption by composites I and II.

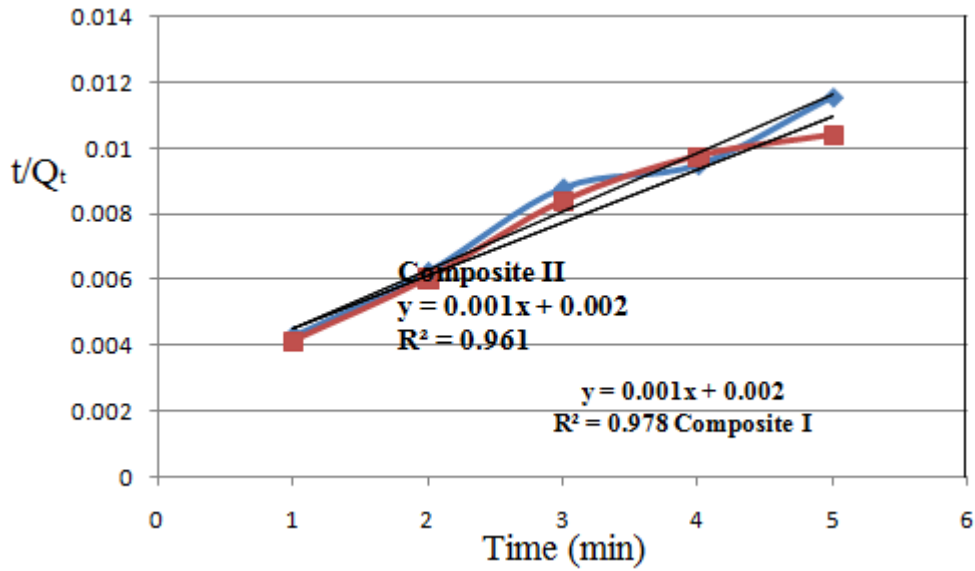


Fig 6. Pseudo-second order plot for MB adsorption by composites I and II.

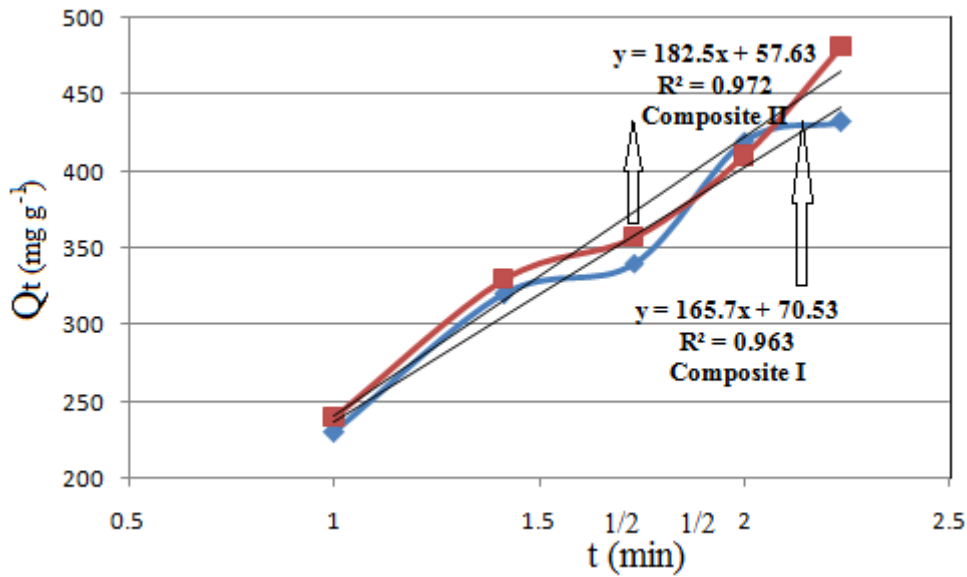


Fig 7. Intraparticle diffusion plot for MB adsorption by composites I and II.

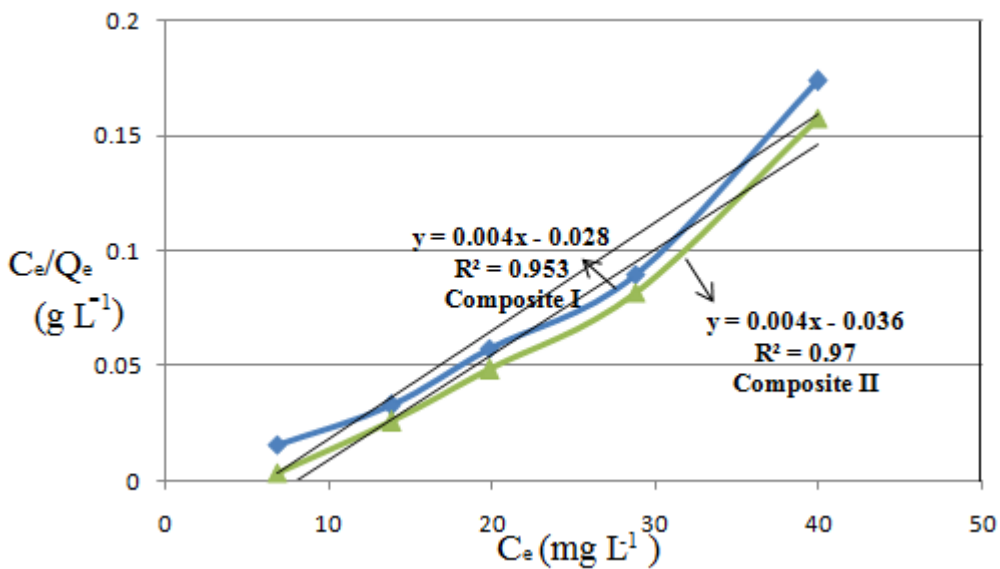


Fig 8. Langmuir isotherm plot for MB adsorption by composites I and II.

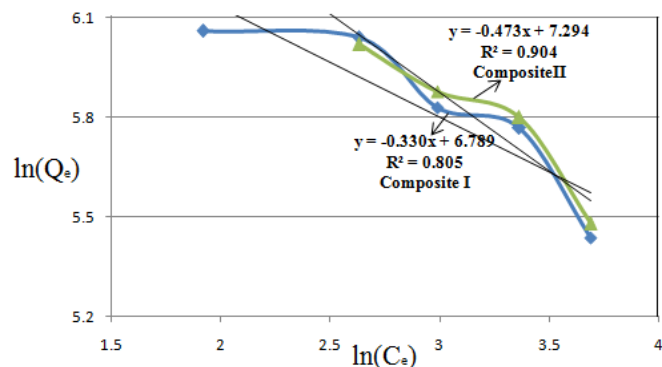


Fig 9. Freundlich isotherm plot for MB adsorption by (a) composites I and II.

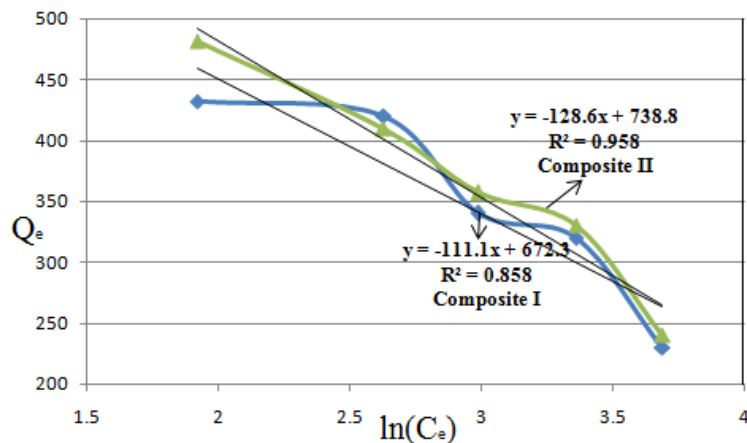


Fig 10. Tempkin isotherm plot for MB adsorption by composites I and II.

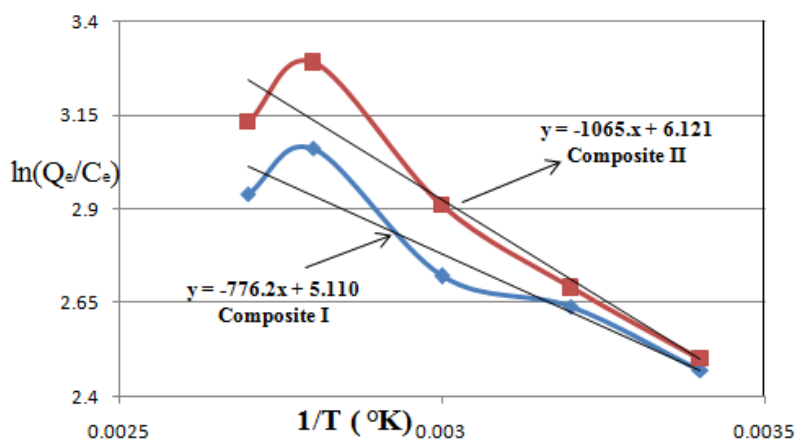


Fig 11. Plot to determine thermodynamic parameters of MB adsorption by composites I and II.

Table 1. Efficiency removal and maximum adsorption capacities of composite I and composite II towards MB

Time (min)	Maximum adsorption capacity (mg g ⁻¹)		Efficiency Removal (%)		Maximum adsorption capacity (mg g ⁻¹)		Efficiency Removal (%)	
	Filter Paper	Composite I	Filter Paper	Composite I	Activated Carbon	Composite II	Activated Carbon	Composite II
1	140	230	44	60	86	240	56	66
2	148	320	56	64	90	330	60	68
3	163	340	60	71	92	357	63	74
4	220	420	65	78	94	418	65	88
5	243	432	66	87	99	481	66	96

Table 2. Maximum adsorption capabilities for MB by different adsorbents

Adsorbents	Adsorption capability (mg g ⁻¹)	C ₀ (mgL ⁻¹)	Reference
Metalloporphyrin	110.53	50	[37]
Polyaniline Magnetite composite	61.51	400	[38]
Polyaniline coated gold-aryl nanocomposite	312	480	[39]
Polypyrrole/sawdust composite	34.36	50	[40]
Graphene oxide/calcium alginate composites	182	80	[4]
Activated Carbon (Ficus Caria Bast)	47.62	70	[9]
Activated Carbon (Surfactant modified)	220	50	[15]
ZnCl ₂ activated carbon	463	50	[13]
Biomass-based activated Carbon	769	50	[2]
Graphene based Mg Silicate	592.2	50	[41]
Pinecone biomass	110	40 (PPmL ⁻¹)	[42]
nMn-bamboo composite	322	140	[43]
Graphene-polypyrrole composite	270	100	[44]
Nickel alginate/activated carbon	505	8.3	[10]
Chitosan-g-polyacrylic acid montmorillonite composite	186	200	[23]
Black Zeolites	57.64	50	[45]
Magnetite porous carbons	306	50	[46]
PANI (Emeraldine Base)	413	50.5	[21]
PANI-Nitroprusside Composite	497	50.5	[21]
Mesoporous Carbons (Peach Stones)	444	200	[6]
Molybdenum dicarbonate	135	50	[Present study]
Molybdenum dicarbonate- filter paper composite	432	50	[Present study]
Molybdenum dicarbonate- activated carbon	481	50	[Present study]

Table 3. Effect of initial concentration (C₀) of MB on the adsorption by Composite I and Composite II

C ₀ (mg L ⁻¹)	50	60	70	80
Adsorbent	Adsorption %			
Composite I	87.00	84.14	81.45	77.30
Composite II	96.25	95.23	94.37	91.20

Table 4. Effects of solution pH on adsorption percentage of MB onto composite I and composite II

pH	2	4	7	10	12
Composite I	65.20	72.12	87.00	76.24	75.12
Composite II	75.34	85.17	96.25	80.60	78.14

Table 5. Effects of Temperature on the adsorption of MB onto composite I and composite II

Adsorption capacity (mg g ⁻¹)	Temperature				
	20°C	40°C	60°C	80°C	100°C
Composite I	432	435	440	443	388
Composite II	481	485	489	494	394

Table 6. Kinetic Parameters for MB adsorption by composite I and II.

Materials	Type	Parameters		
	Pseudo-first order kinetics	$k_1(\text{min}^{-1})$	$Q_e(\text{mgg}^{-1})$	R^2
Composite I		0.4675	607	0.991
Composite II		0.5158	582	0.993
Materials	Pseudo-second order kinetics	$k_2(\text{min}^{-1})$	$Q_e(\text{mgg}^{-1})$	R^2
	Composite I	5×10^{-4}	1000	0.978
Composite II		5×10^{-4}	1000	0.961
Materials	Intra-particle diffusion model	$k_i(\text{g}(\text{mg min}^{-1}))$	$C_e(\text{mgL}^{-1})$	R^2
	Composite I	165.7	70.53	0.963
Composite II		182.5	57.63	0.972

Table 7. Parameter values of different adsorption models (calculated after linear fit method).

Materials	Langmuir Model			Freundlich		Tempkin	
	Q_{max}	K_L	R^2	$K_F(\text{Lg}^{-1})$	R^2	$K_T(\text{Lmg}^{-1})$	R^2
Composite I	250	0.142	0.953	6.16×10^6	0.805	1.12×10^6	0.858
Composite II	250	0.111	0.97	19.68×10^6	0.904	5.49×10^5	0.958

Table 8. Thermodynamic parameters for the removal of MB by composites I and II

Adsorbent	$\Delta G^\circ (\text{J mol}^{-1})$				$\Delta H^\circ (\text{J mol}^{-1})$	$\Delta S^\circ (\text{J K}^{-1} \text{mol}^{-1})$
	20°C	40°C	60°C	80°C		
Composite I	-5994	-6418	-7693	-8542	6453	42.48
Composite II	-6132	-7149	-8167	-9085	8779	50.89

5. References

- [1] Freshwater Resources, National Geographic Society & education.nationalgeographic.org.
- [2] N U M. Nizam NUM, M. M. Hanafiah MM, E. Mahmoudi E, A. A. Halim AA and A. W. Mohammad AW, 2021, Scientific Reports, 11 (2021) 8623-8640.
- [3] E. Okoniewska E, Sustainability, 13 (2021) 4300-4312.
- [4] Y. Li Y, Q. Du Q, T. Liu T, J. Sun J, Y. Wang Y, S. Wu S, Z. Wang Z, Y. Xia Y, L. Xia L, 2013, Carbohydrate Polymers 95 (2013) 501– 507.
- [5] Abate et al. 2020, Environmental System Research, 9 (2020) 29-42.
- [6] S. Álvarez-Torrellas S, R. García-Loverab R, A. Rodríguez A, J. García J, 2015, Chemical Engineering Transactions, 43 (2015) 1963-1968.
- [7] P. R. Evora PR and F. Viaro F, (2006), Curr Drug Targets, 7(9) (2006) 1195-204.
- [8] P. R. Evora PR et al (2015), Rev Bras Cir Cardiovasc. 30(1) (2015) 84-92.
- [9] D. Pathania D, S. Sharma S, P. Singh P, Arabian Journal of Chemistry, (2013)1-7. <http://dx.doi.org/10.1016/j.arabjc.2013.04.021>.
- [10] Y. Wang Y, J. Pan J, Y. Li Y, P. Zhang P, M. Li M, H. Zheng H, X. Zhang X, H. Li H and Q. Du Q, Journal of Material Research and Technology, 9(6) (2020) 12443–12460.
- [11] T. Etemadinia T, A. Allahrasani A and B. Barikbin B, Polymer Bulletin, 76(12) (2019) 6089-6109.
- [12] S. N. Hurairah SN, N. M. Lajis NM, A. A. Halim AA, Journal of Geoscience and Environment Protection, 2020, 8, 128-143.
- [13] M. Khodaie M, N. Ghasemi N, B. Moradi B and M. Rahimi M, Journal of Chemistry, (2013)1-6. <http://dx.doi.org/10.1155/2013/383985>.
- [14] P. K. Malik PK, Journal of Hazardous Materials B113 (2004) 81–88.
- [15] Y. Kuang Y, X. Zhang X and S. Zhou S, Water, 12 (2020) 587-605.
- [16] Jayachandran Sheeja J, Krishnan Sampath K and Ramasamy Kesavasamy R, Adsorption Science and Technology, (2021) 1-12. <https://doi.org/10.1155/2021/5035539>.
- [17] M. Stan M et al. Synthetic Metals, 288 (2022) 117117.
- [18] S. Karthi S, R. K. Sargeetha RK, K. Arumugam K, T. Karthitta T and S. Umala S, Materials Today: Proceedings, 66(4) (2022) 1945-1950.
- [19] W-D Xiao WD et al. International Journal of Biological Macromolecules, 218 (2022) 285-294.
- [20] H. Li H, V. L. Budarin VL, J. H. Clark JH, M. Noth M and X. Wu X, Journal of Hazardous Materials, 436 (2022) 129174.
- [21] F. A. Rafiqi FA and K. Majid K, Journal of Material Sciences, 52(11) (2017) 6506-6524.
- [22] F. A. Rafiqi FA and K. Majid K, Journal of Environmental Chemical Engineering, 3(4) (2015) 2492-2501.

- [23] L. Wang L, J. Zhang J, A. Wang A, *Colloids and Surfaces A: Physicochemical and Engineering aspects*, 322 (2008) 47-53.
- [24] J. Yan J and R. Xu R, *Bioresources*, 10 (2015) 4065-4076.
- [25] A.M. Youssef AM, S. Kamel S, M. El-Sakhawy M, M.A. E Samahy MAE, *Carbohydrate Polymers*, 90 (2012) 1003-1007.
- [26] M. Liu M, S. He S, W. Fan W, Miao Yue-E and T. Liu T, *Composites Science and Technology*, 101 (2014) 152-158.
- [27] T. K. Sen TK, S. Afroze S, H. M. Ang HM, *Water Air Soil Pollution*, 218 (2011) 499.
- [28] S. Zhou S et al. *Carbohydrate Polymers*, 258(2021) 117690-117699.
- [29] H. Bian H, Y. Yang Y and P. Tu P, *Bioresources*, 16(4) (2021) 8353-8365.
- [30] X. Li X, W. Liu W, Mengjuan Li M, Y. Li Y, Mi. Ge M, *Polymer Composites*, 35 (2014) 993-998.
- [31] H. A. Hamid HA et al. *Progress in Engineering Applications and Technology*, 1(2020) 116-126.
- [32] A. Szyman´ska A, W. Nitek W, M. Oszejca M, W. Łasocha W, K. Pamin K and J. Połtowicz J, *CatalLett*, 146 (2016) 998-1010.
- [33] R. K. Dev RK, A. Bhattarai A, N. K. Chaudhary NK and P. Mishra P, *Int. J. Pharm. Sci. Rev. Res.*, 60(1) (2020) 115-121.
- [34] R.B. Rastogi RB and M. Yadav M, *Tribology International* 36 (2003) 511-516.
- [35] https://en.m.wikipedia.org/wiki/Ammonium_tetrathiomolybdate.
- [36] H. N. Abdelhamid HN, A. P. Mathew AP, *Carbohydrate Polymers*, 274 (2021) 118657-63.
- [37] M. M. Almoneef MM, J. Roubeh J and M. Mbarek M, *Synthetic Metals*, 290 (2022) 117158.
- [38] D. D. A. Buelvas DDA et al. *Synthetic Metals*, 292 (2023) 117232.
- [39] B. A. AlMashrea BA et al. *Synthetic Metals*, 269 (2020) 116528-116540.
- [40] R. Ansari R, Z. Mosayebzadeh Z, *Journal of the Iranian Chemical Society*, 7 (2010) 339-350.
- [41] A. Que, T. Zhu & Y. Zheng, *J Mater Sci* 56, (2021) 16351-16361.
- [42] J. D. Xiao JD, L. G. Qiu LG, X. Jiang X, Y. J. Zhu YJ, S. Ye S, X. Jiang X, *Carbon*, 59 (2013) 372.
- [43] S. E. Shaibu SE, F. A. Adekola FA, H. I. Adegoke HI, O. S. Ayanda OS, *Materials*, 7 (2014) 4493-4507.
- [44] L. Bai L, Z. Li Z, Y. Zhang Y, T. Wang T, R. Lu R, W. Zhou W, H. Gao H, S. Zhang S, *Chemical Engineering Journal*, 279 (2015) 757-766.
- [45] M. M. Selim, D.M. EL-Mekkawi, F. A. Ibrahim, *J. Mater Sci*, 53 (2018) 3323-3331.
- [46] J. D. Xiao JD et al. *Carbon*, 59 (2013) 372-382.
- [47] L. Bai L et al., *Chemical Engineering Journal*, 279 (2015) 757-766.
- [48] W. Wang W et al., *Applied Surface Science*, 346 (2015) 348-353.